Differential Decay of Multiple eNA Components from a Cetacean

Pedro FP Brandão-Dias[1]; Megan Shaffer[1]; Gledis Guri[1]; Kim M Parsons[2]; Ryan P Kelly[1]; Elizabeth Andruszkiewicz Allan[1]

1: School of Marine and Environmental Affairs, University of Washington, Seattle, 98105, Washington, USA

2: Conservation Biology Division, Northwest Fisheries Science Center, National Marine Fisheries Service, National Oceanic and Atmospheric Administration, Seattle, 98112, Washington, USA

ABSTRACT

Environmental nucleic acids (eNA), such as DNA and RNA, are powerful tools for monitoring biodiversity. Yet, interpreting eNA detections requires understanding their environmental persistence—especially in marine systems and for rare taxa like marine mammals, where decay rates remain largely unquantified. We conducted a controlled decay experiment using seawater from an open dolphin enclosure to track degradation of six eNA components derived from *Tursiops truncatus*: mitochondrial eDNA of varying lengths, ribosomal eRNA, and messenger eRNA. Using digital droplet PCR (ddPCR), we quantified each target over seven days and found that decay followed a biphasic exponential pattern, with rapid initial loss (~48 hours at 15 °C) followed by slower secondary decay. Cytb messenger eRNA degraded the fastest, becoming undetectable within four hours. Ribosomal eRNA was more persistent, decaying slightly faster than its DNA counterpart (λ_1 = 0.125 vs. 0.105 hr^{-1}). Longer eDNA fragments decayed more rapidly (λ_1 = 0.121 hr^{-1}) than shorter ones (λ_1 = 0.083 hr^{-1}). These findings support the use of eDNA fragment length as a proxy for degradation state and suggest that combining multiple eNA components with distinct stabilities—such as ribosomal eRNA and eDNA of varying fragment lengths—can provide a molecular clock framework for inferring the age of detected eDNA. This approach improves the spatiotemporal resolution of eNA-based monitoring, particularly for elusive or rare species that act as point sources. We also emphasize the importance of explicitly distinguishing between RNA types (ribosomal vs. messenger) in environmental studies, given their divergent stability and ecological interpretability.

KEYWORDS: Removal, ddPCR, Bayesian, Experimental, Marine Mammal

INTRODUCTION

Environmental DNA (eDNA) and, more recently, environmental RNA (eRNA)—collectively referred to as environmental nucleic acids (eNA)—have emerged as powerful tools for ecological monitoring and biodiversity assessments (Bowers et al., 2021; Takahashi et al., 2023; Yates et al., 2021). Unlike traditional direct observation methods, eNA-based surveys rely on indirect detection of species through trace amounts of genetic material that organisms release into their environment (Barnes & Turner, 2016; Power et al., 2023). Due to the nature of eNA accumulation in space, eNA surveys are fundamentally integrative, containing genetic information accumulated over time rather than providing an instantaneous snapshot. This integrative property enhances detection sensitivity compared to nets or visual surveys which may integrate over space but reflect a single point in time; that is, they are snapshot-based methods, making eNA detection analogous to a short movie rather than a single photographic frame. However, the extent to which eNA surveys integrate species presence over both time and space depends on several environmental and molecular factors that govern its persistence and movement, thus making the integration variable (Allan et al., 2021) .

Accurately interpreting eNA detections requires understanding how much time and space is integrated into each detection event. This, in turn, demands detailed knowledge about the origin, state, transport, and persistence (or decay) of nucleic acids within the environment, collectively referred to as the ecology of eNA (Barnes & Turner, 2016; Harrison et al., 2019). Among these processes, the decay rate of eNAs has been among the most frequently estimated parameters (e.g. Barnes et al., 2014; T. Jo et al., 2020; Scriver et al., 2023). The prominence of decay rate studies stems not only from the relative ease of estimating decay rates compared to transport or production, but also from the fundamental role decay plays in determining the temporal resolution of eNA surveys. While transport primarily governs the spatial resolution of detections (J. Xiong et al., 2025)—largely shaped by hydrological, oceanographic, or atmospheric processes— decay dictates how long genetic signals remain detectable, helping set the temporal bounds of the eNA movie, which reflects a steady-state balance among production, transport, and degradation.

Beyond simply establishing an upper temporal limit for eNA detection, certain applications require more precise aging of the biological source of detections within a sample. This is particularly relevant for point sources or rare detections, such as those of marine mammals (Suarez-Bregua et al., 2022) or invasive species (Jerde et al., 2011; Xia et al., 2018). To address this, previous research has proposed using the ratio of eRNA to eDNA as a "molecular clock" for eNA persistence (Marshall et al., 2021). Since eRNA generally degrades faster than eDNA, qualitatively, a sample with a high proportion of eRNA to eDNA

suggests a recent biological source, whereas a sample containing only eDNA indicates an older signal (Marshall et al., 2021; Scriver et al., 2023). This is analogous to applications in the forensic literature, where the ratio of presence between messenger RNA and DNA, as well as the degradation state of RNA, can be reliably used to infer time since death (Sampaio-Silva et al., 2013).

Nonetheless, this framework extends beyond eDNA/eRNA ratios to any eNA component with distinct degradation rates. Environmental nucleic acids exist in multiple molecular forms, including intracellular, particle-adsorbed, dissolved, nuclear, mitochondrial, and other fractions (Kirtane et al., 2023; Mauvisseau et al., 2021; Nagler et al., 2022). Provided these components decay at different rates, then their relative proportions over time and space provide a molecular signature for estimating detection age (Brandão-Dias et al., 2023). Naturally, this approach can be applied not only to molecular forms of eDNA, but also to experimentally defined fractions such as fragment lengths assessed through multiple genetic markers (Bylemans et al., 2018; T. Jo, Murakami, et al., 2020), variations in eNA particle size distributions captured by sequential filtration (Brandão-Dias et al., 2025; T. Jo et al., 2019; Zhao et al., 2021), differences between eNA extracted from distinct environmental media, such as sediment versus water (Sakata et al., 2020), eDNA to eRNA ratios (Marshall et al., 2021), among many others.

In theory, the most effective molecular components for estimating detection age are those with strongly contrasting decay rates, as their relative proportions shift measurably over short timescales, thus enhancing spatiotemporal resolution. However, in practice, the choice of eNA components must balance temporal sensitivity with logistical and methodological feasibility. Numerous studies have measured eNA decay rates, consistently highlighting that these rates are highly context dependent. Decay dynamics vary substantially with environmental conditions such as biological activity and temperature (Joseph et al., 2022; Lamb et al., 2022), depend on target organism (Andruszkiewicz Allan et al., 2021), and differ significantly due to methodological differences such as filter pore size and molecular marker length (Brandão-Dias et al., 2023; Brandão-Dias et al., 2025; T. Jo et al., 2017; Zhao et al., 2021). Consequently, generalizing decay rates across systems or conditions is challenging, especially since controlled experimental setups seldom fully represent the complexities of natural environments. As a result, accurate molecular time inference requires decay estimates tailored to or closely approximating the specific environmental conditions and molecular targets of interest.

In freshwater systems, multiple studies have compared eRNA and eDNA decay, generally finding that eRNA—particularly messenger RNA (emRNA)—decays more rapidly than eDNA (e.g. T. Jo et al., 2023; Kagzi et al., 2022). In marine environments, however,

relatively few studies have directly compared eRNA and eDNA decay. For example, Qian et al. (2022) observed significantly faster decay of prawn-derived emRNA compared to eDNA, particularly under colder temperatures. Conversely, Wood et al. (2020) examined decay rates of worm- and tunicate-derived emRNA, finding only slightly elevated decay rates compared to eDNA. Similarly, Scriver et al. (2024) found no significant difference in decay between emRNA and eDNA from marine worms. To date, no studies have directly assessed decay rates of ribosomal eRNA (erRNA) in marine environments, although Miyata et al. (2021) noted that erRNA yielded more ecologically relevant metabarcoding detections than eDNA, suggesting greater transience and thus potentially faster decay. Crucially, despite this emerging body of work on eRNA, no studies have yet evaluated the decay rates of eNA components, eDNA or eRNA, specifically derived from marine mammals.

Here, we experimentally assessed the differential decay rates of multiple eNA components from the common bottlenose dolphin, *Tursiops truncatus* (Montagu, 1821). Using seawater sourced from an open environment, netted dolphin enclosure, we conducted a controlled decay experiment, tracking the persistence of eDNA of several molecular lengths, emRNA, and erRNA over time. We hypothesized that eRNA would degrade faster than eDNA, with emRNA decaying the fastest due to its transient nature. We expected erRNA to persist longer than emRNA due to its structural properties, but still degrade more rapidly than eDNA. Lastly, we anticipated that larger DNA fragments would decay faster than shorter ones, following previous findings (Brandão-Dias et al., 2025; Hirohara et al., 2021) and known fragmentation patterns. By quantifying these decay rates, we aimed to improve the temporal resolution of marine mammal detections and refine our understanding of eNA persistence in marine environments.

METHODS

Environmental DNA source and decay experiment

A small, managed group of non-native Atlantic bottlenose dolphins (*Tursiops truncatus*) is housed in a defined area along the eastern bank of Hood Canal, Washington, as part of the U.S. Navy's Marine Mammal Program. These dolphins frequently inhabit netted enclosures adjacent to a pier, where seawater freely exchanges with the surrounding marine environment. For this study, in October 2024 we collected water from within one of these netted enclosures containing a single dolphin at the time of sampling. Using a 2-liter pitcher, we filled three replicate 25-liter carboys, which served as the three biological replicates for the decay study (Figure 1A). To minimize contamination, collectors wore gloves during

140 sampling, and both the pitcher and carboys had been cleaned overnight with 1% bleach and
141 extensively rinsed with deionized water before use.

142 After collection, water within each carboy was mixed, and a 2-liter baseline sample
143 was filtered from each carboy to assess initial eNA concentrations before transport. These
144 samples were immediately filtered and preserved (see below for filtration and preservation
145 details). The carboys were then sealed and transported at ambient temperature to the
146 laboratory and an environmental chamber for the decay experiment. Temperature loggers
147 placed inside one of the carboys recorded transport temperatures ranging from 16°C to 12°C
148 over the course of ~3 hours of transport back to the laboratory.

149 At the laboratory, the three biological replicate carboys were decontaminated
150 externally with bleach before being placed inside an environmental chamber, where they
151 remained for the duration of the experiment. A fourth carboy, filled with deionized (DI) water,
152 was also placed in the environmental chamber as a cross-contamination control. The
153 environmental chamber was maintained at a constant 15°C with a 16-hour daylight cycle
154 throughout the experiment. To ensure water circulation, we inserted air hoses with stones
155 powered by a Whisper 100 (Tetra) into each carboy, in addition to a U-shaped plastic
156 sampling hose, both of which remained in place for the entire experiment. Like the carboys,
157 each of those were cleaned by overnight 1% bleach bath and extensively rinsed with
158 deionized water before use.

159 To evaluate the decay of eNA over time, 2-liter water samples were collected from
160 each carboy at nine timepoints: 0, 4, 8, 12, 24, 48, 96, 140, and 188 hours (Figure 1A). At each
161 timepoint, aeration was temporarily turned off to prevent aerosolization, and water was
162 drawn via the plastic sampling hoses (Figure S1A). We used sequential filtration to capture
163 eDNA across different particle sizes. Each sample was filtered through a tandem system of
164 three filter housings (Smith-Root, non-self-preserving) equipped with 5 µm, 1.0 µm, and 0.45
165 µm mixed cellulose ester (MCE) 47 mm filters (Advantec), each backed by polyester drain
166 disks (Sterlitech). Filters were connected downstream to an eDNA Citizen Science Sampler
167 (Smith-Root) for vacuum filtration. Immediately after filtration, filter housings were opened,
168 and sterilized forceps were used to fold each filter twice, sample side in, before placing it
169 into 5 mL Lo-Bind tubes (Eppendorf) containing 2 mL of DNA/RNA Shield (Zymo). Samples
170 were incubated at room temperature for 30 minutes, then frozen at -80°C until DNA
171 extraction within one month.

172 To prevent cross-contamination, all forceps, filter holders, adapters, and tubing were
173 submerged in 5% bleach baths, thoroughly rinsed with deionized (DI) water, and dried before
174 reuse. Two independent sets of filtration equipment were available, allowing for alternating
175 use between timepoints. Additionally, at the end of each timepoint, we filtered 2 liters of the

DI water used for post-bleach rinsing through a 0.45 µm filter as a contamination control to verify the effectiveness of our decontamination procedures.

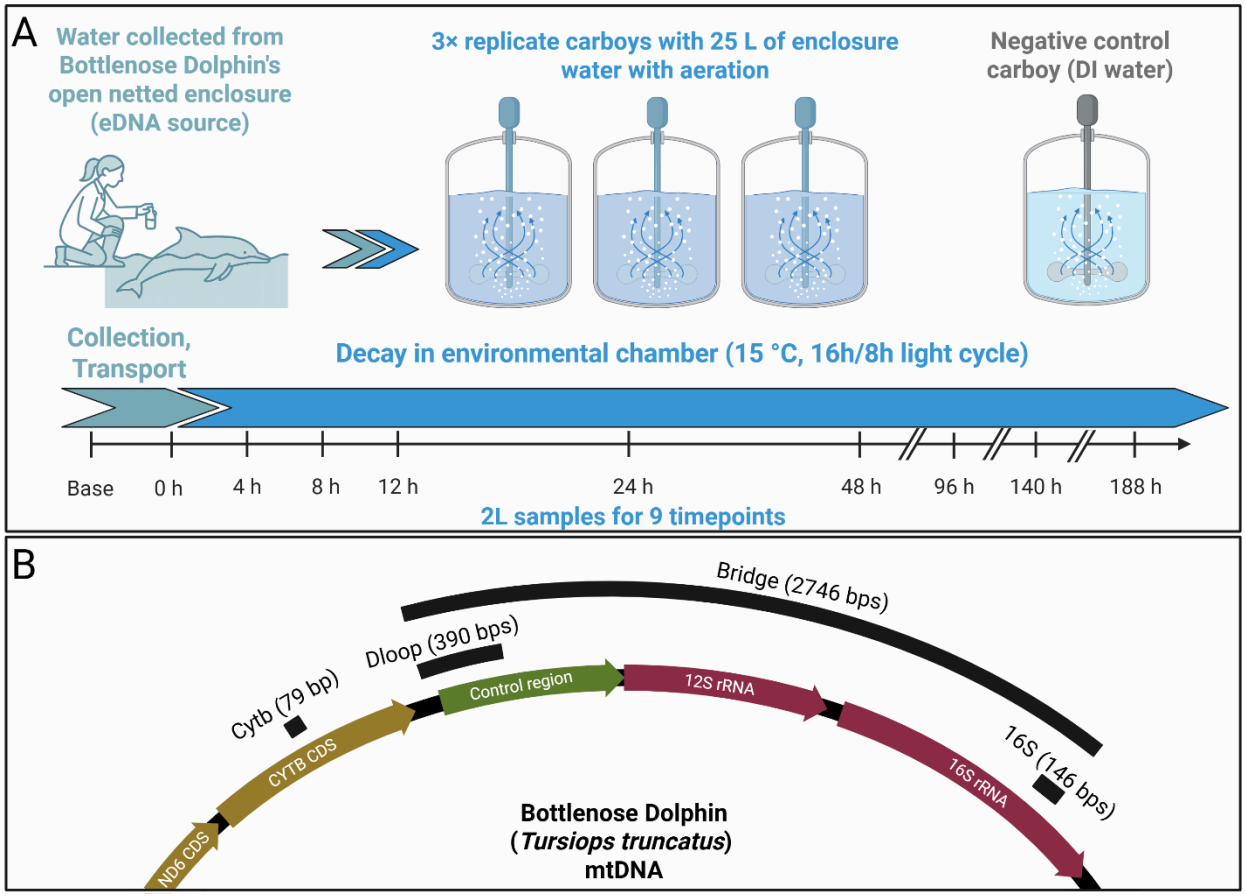

Figure 1: Overview of the experimental design and the four mitochondrial targets quantified. (A) Water-decay experiment. Seawater was scooped from inside an open-net enclosure housing an Atlantic bottlenose dolphin (*Tursiops truncatus*) and poured into three 25 L carboys (biological replicates). A fourth carboy containing de-ionized (DI) water served as cross-contamination control. Carboys were held in a 15 °C environmental chamber with continuous aeration and a 16 h light / 8 h dark cycle. Two-liter subsamples were withdrawn at nine timepoints (0–188 h) for size-fractionated filtration and downstream DNA/RNA extraction. (B) Locations of the mitochondrial assays. Arrows show the relative positions of the 79 bp Cytb amplicon (protein-coding), the 390 bp D-loop amplicon (non-coding control region), and the 146 bp 16 S rRNA amplicon (ribosomal) on the circular dolphin mtDNA. The 2746 bp segment spanning D-loop to 16 S (black arc labelled "Bridge") represents the minimum intact bridging fragment between 16S and Dloop loci.

DNA and RNA extraction

193 Nucleotides were extracted from samples using a two-step process. First, frozen
194 filters with buffer were thawed and incubated with agitation at 37 °C for ~15 minutes to
195 dissolve any precipitation. The samples were then thoroughly vortexed, and the buffer (2 mL)
196 was transferred to an Amicon Ultra-15 30 kDa centrifugal filter unit (Millipore-Sigma) and
197 centrifuged at 4,000 rpm for 30 minutes, concentrating the buffer to ~400 µL. Both eDNA and
198 eRNA were extracted simultaneously using the Quick DNA/RNA Miniprep Kit (Zymo
199 Research), following the manufacturer's protocol with a 30-minute proteinase K incubation
200 before adding the binding buffer.

201 This extraction process results in two sequential extracts (Figure S2A). The first
202 primarily contains the DNA (hereafter "eDNA"), whereas the second is expected to contain
203 RNA; however, empirical results showed that it also contained a substantial amount of DNA,
204 hereafter referred to as "carryover eDNA". One-third of this second extract —containing both
205 eRNA and carryover eDNA— was retained for carryover eDNA analysis (see supplement,
206 Figures S2, S3), while the remaining two-thirds were treated with ezDNAse (ThermoFisher
207 Scientific) at 37 °C for 30 minutes to remove the carryover DNA in preparation for cDNA
208 synthesis.

209 The DNAse-treated portion of the extract was subjected to a SuperScript IV
210 (ThermoFisher Scientific) first-strand cDNA synthesis reaction using random hexamers in
211 the denaturation step following the manufacturer's protocol, to convert RNA into cDNA. This
212 product is hereafter referred to as "eRNA." Each sample was also subjected to a second
213 control reaction, identical in components and cycling conditions, but without the reverse
214 transcriptase enzyme. This reaction product is hereafter referred to as the "No-RT," and it was
215 used to assess post-DNAse treatment carryover eDNA, ensuring that quantifications from
216 the eRNA extract were from eRNA-derived cDNA rather than residual carryover eDNA. For
217 details on carryover eDNA analysis, see the supplementary material.

218

219 **Target eNA quantification**

220 Target eNA were quantified using three assays, all of which target mitochondrial loci
221 (Table 1). The first was a 79 bp fragment of *Cytochrome b* (Cytb), a protein-coding gene, from
222 which we quantified three components: eDNA, messenger eRNA (hereafter emRNA), and
223 the No-RT control. The second was a 146 bp fragment of the *16S* ribosomal RNA gene, used
224 to quantify eDNA, ribosomal eRNA (erRNA), and No-RT control. The third was a 390 bp
225 fragment of the *D-loop* control region, from which only eDNA was analyzed as it is a non-
226 coding region.

227 In addition to these three markers quantified directly by their respective primers and
228 assays, a fourth mitochondrial DNA (mtDNA) component—referred to as the "16S-Dloop
229 bridge sequence", hereafter "Bridge" for short—was quantified within the duplex ddPCR
230 reaction targeting both *16S* and *D-loop*. This Bridge signal arises from intact (2746+ bps)
231 mtDNA molecules that physically link the two markers (Figure 1B, see details below and in
232 the supplement). Altogether, this yielded six distinct eNA components to be analyzed: Cytb
233 eDNA, Cytb emRNA, 16S eDNA, 16S erRNA, Dloop eDNA, and Bridge eDNA (Table 2).

234 All markers were quantified using digital droplet PCR (ddPCR). Cytb eDNA, Cytb
235 emRNA, Cytb No-RT, 16S erRNA and 16S No-RT were quantified using monoplex reactions.
236 Each 22 µL reaction contained 11 µL of ddPCR Supermix for Probes (Bio-Rad Inc., Hercules,
237 CA), 250 nM of probe, 900 nM of each primer (IDT), and 2 µL of template extract. The
238 thermocycling conditions were: 4°C for 10 min; 95°C for 10 min; 45 cycles of 94°C for 30 s
239 and 60°C for 60 s (annealing/extension); followed by 98°C for 10 min and a final hold at 4°C.

240 For *16S* and *D-loop* eDNA, we used a duplex ddPCR reaction. Each 22 µL reaction
241 included 11 µL of Supermix, 900 nM of *D-loop* primers, 600 nM of *16S* primers, 250 nM of
242 each probe, and 2 µL of extract. Given the longer amplicon sizes, we adjusted cycling
243 conditions: 4°C for 10 min; 95°C for 10 min; 44 cycles of 94°C for 30 s, 56°C for 30 s
244 (annealing), and 72°C for 120 s (extension); followed by 98°C for 10 min and a 4°C hold. This
245 duplex design allowed us to simultaneously quantify 16S, D-loop, and the mtDNA bridge
246 between them (Figure 1B).

247 As mentioned above, this duplex reaction also allowed us to quantify a fourth marker,
248 Bridge, given by ddPCR droplet sorting and linkage between markers. Droplet PCR partitions
249 the reaction into ~20,000 droplets, enabling absolute quantification of target molecules
250 using Poisson statistics. If targets are unlinked, they sort into droplets independently, and
251 double-positive droplets arise randomly. However, due to the circular nature of mtDNA, *16S*
252 and *D-loop* are physically linked in intact molecules. The shortest span between them is
253 2746 bp, though linkage could span the full ~16,388 bp mitochondrial genome (Louis et al.,
254 2023; Xiong et al., 2009). Thus, in a hypothetical situation where all mtDNA molecules are
255 intact in the sample, all droplets containing 16S would automatically also contain Dloop,
256 and vice versa, making all droplets positive for both markers.

257 However, because eDNA in environmental samples is partially fragmented, droplets
258 in the duplex assay include a mixture of single-positive and double-positive events. Double-
259 positive droplets can arise from two mechanisms: (1) random co-localization of
260 independently degraded DNA fragments containing 16S and D-loop sequences, or (2) intact
261 DNA molecules physically bridging the two markers (i.e., ≥2746 bp). Using the counts of
262 single-positive droplets for each marker, one can calculate the expected number of double-

263 positive droplets that would result from mechanism (1) alone. This expected value is then
264 subtracted from the observed number of double-positive droplets, and the remainder is
265 attributed to mechanism (2), providing an estimate of the number of intact, bridged
266 molecules. See supplements for full derivation and schematics.

267 For all ddPCR assays, droplets were generated using the AutoDG Droplet Generator
268 (Bio-Rad Inc.), thermocycling was performed on C1000 Touch Thermal Cyclers (Bio-Rad
269 Inc.), and droplet fluorescence was read using a QX200 Droplet Reader (Bio-Rad Inc.). Each
270 plate included one positive control and three no-template controls (NTCs), used to define
271 positive thresholds and screen for contamination.

272 Finally, to confirm the absence of non-target marine mammals in the decay
273 experiment, we opportunistically performed metabarcoding on eDNA samples filtered at the
274 first timepoint of each carboy. We detected no other cetacean species in the decay water
275 (Tables S1, S2). Details of metabarcoding methods and results are provided in the
276 Supplement.

277

278 **Table 1: Oligonucleotide sequences for the assays used herein.**

Mitochondrial locus	**Oligo Name**	**Role**	**Sequence**	**Reference**
Cytochrome b (Cytb)	Ttru-cytb_F	Forward	TTATTCTTCCATTCATCATCAC	Xiong et al., 2025
	Ttru-cytb_R	Reverse	GTGGGGTTGTTGGATCCTGT	Xiong et al., 2025
	Ttru-cytb_P	Probe	/5FAM/AATAGTAGG/ZEN/TGAACGGCTGCCA/3IABkFQ/	This study
16S	Ttru-16S_F	Forward	AGGGTTTTACTGTCTCTTACTCTT	This study
	Ttru-16S_R	Reverse	CTTTGTTATCCCTTGGTGGTATTA	This study
	Ttru-16S_P	Probe	/5-HEX/ATAATGCAA/ZEN/TAAGACGAGAAGACCCTATGG/3IABkFQ/	This study
Dloop (Control region)	DL1-HL_F	Forward	CACCCAAAGCTGRARTTCTDYATAAACT	This study
	Oordlp4	Reverse	GCGGGTTGCTGGTTTCACG	Baker et al., 2018
	Ttru-DL_P	Probe	/5FAM/ACTGACGTA/ZEN/GTACTGTGATGTTGTGGTAACTGTAC/3IABkFQ/	This study

279

280

281 **Table 2: Markers analyzed herein.** “Bridge” refers to the 16S-Dloop bridge sequence (Figure 1B).

Mitochondrial locus	**Nucleotide type**	**Extract**	**Assay**	**Target length (base pairs)**
Cytb	DNA	eDNA	Cytb monoplex	79
Cytb	mRNA	eRNA	Cytb monoplex	79
16S	DNA	eDNA	16S-Dloop duplex	146
16S	rRNA	eRNA	16S monoplex	146
Dloop	DNA	eDNA	16S-Dloop duplex	390
Bridge	DNA	eDNA	16S-Dloop duplex*	2746-16390

282

283 * See supplement for calculation details

Statistical analysis and decay rate estimation

We built a Bayesian hierarchical model to jointly estimate the eNA concentrations and the decay rates for each component and marker from the observed ddPCR droplet counts. To estimate the eNA concentrations from ddPCR droplet reader observations, we followed the same approach used by Guri et al. (2024): we modeled the observed number of positive droplets W_i as a Binomial distribution:

$$W_i \sim \text{Binomial}\ (U_i, p_i)$$

Where p_i is the probability that an individual droplet positively amplifying the target locus from the total number of droplets generated U_i.

Given that ddPCR partitioning of the sample follows a Poisson distribution, the event rate corresponding to the eNA molecules (ω) present in the sample *i* (Hindson et al., 2013), we write p_i as a follows:

$$cloglog(p_i) = ln(\omega_i)$$

For inferring the eNA concentration in the mesocosm (C_i; units copies/L) we normalize for the volume filtered, eluted, and diluted as follows:

$$ln(\omega_i) = ln(C_i) - \ ln(rvol) + \ ln(tvol) + ln(d_i) - ln\left(\frac{evol}{filt_i}\right) - \ ln(dpletvol)$$

where *rvol* is the total ddPCR reaction volume (22 µL), $tvol$ is the template volume added to the reaction (2 µL), d_i is a sample-specific template dilution (caused by reverse transcription reaction), *evol* is the extraction eluted volume (50 µL), $filt_i$ is the sample-specific filtered volume, and *dpletvol* is the ddPCR droplet volume (~0.85 nL), as specific by Bio-Rad and used by Guri et al. (2024).

To calculate decay for each of the components and markers, we tested six different decay models, and ultimately used the Biphasic Exponential Decay model which yielded the highest likelihood (see Supplements for model testing). The biphasic exponential decay model assumes two exponential decay phases with a transition time:

$$\mathrm{C(t)} = \begin{cases} \mathrm{C_0} e^{-\lambda_1 \mathrm{t}}, & \mathrm{t} < \mathrm{t_x}, \\ \mathrm{C_x} e^{-\lambda_2 (t - t_x)}, & \mathrm{t} \geq \mathrm{t_x}. \end{cases}$$

where $C(t)$ is the concentration of eNA at time t; C_0 is the initial concentration at t = 0; λ_1 and λ_2 are the decay rate constants for the first and second phases, respectively; t_x is the time where decay rate changes; and C_x is the concentration at t_x determined as $C_x = C_0 e^{-\lambda_1 t_x}$.

The joint model estimates the concentrations C_i for each sample based on two technical replicates, and the decay rates (λ_1 and λ_2) and t_x for each component and marker combination considering all three biological replicates. The model was implemented in the Stan language with the R package Rstan (Carpenter et al., 2017) running four independent Markov chain Monte Carlo (MCMC) chains with 2000 warmup and 4000 sampling iterations.

RESULTS

Controls

All target eNA assays from the fourth (control) carboy, filtration negative controls, extraction blanks, and No-RT controls yielded zero positive droplets, with the exception of occasional single positive droplets in No-RT controls. These rare events indicate minimal residual DNA carryover in RNA extracts despite DNase treatment. To account for this, we subtracted the droplet count observed in each No-RT control from the corresponding eRNA droplet count of the same sample before proceeding with downstream analyses.

Little eDNA found in smaller pore sizes

To assess the particle-size distribution of dolphin eDNA, we filtered each time-point sample through a 3-stage serial filtration system (5 µm, 1.0 µm, 0.45 µm). Preliminary sample screening of the first timepoint samples found that >95% of the Cytb signal was captured on the 5 µm filter at time zero. Therefore, all downstream analyses used this fraction exclusively (Figure 2).

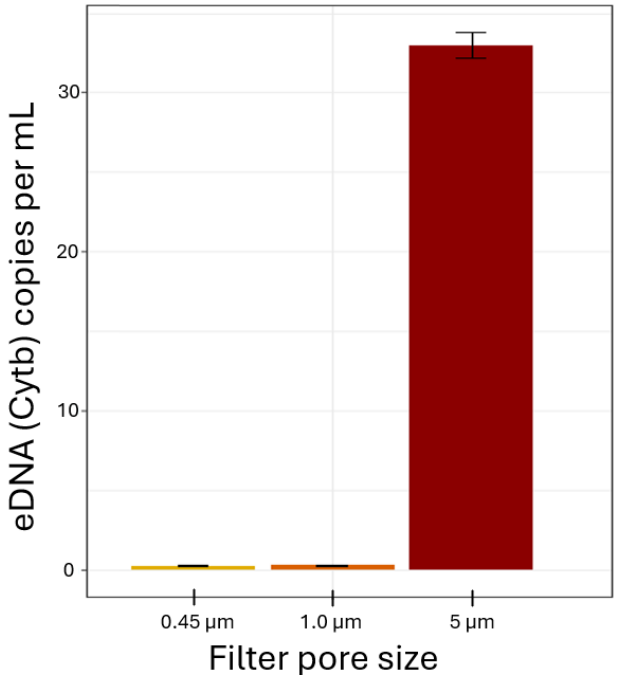

Figure 2: Particle size distribution of Bottlenose Dolphin eDNA in the first timepoint. Concentration of dolphin mitochondrial Cytb eDNA recovered at the first sampling time-point as a function of pore size. Filters with pore sizes < 5 µm retained negligible eDNA, so subsequent analyses rely exclusively on extracts from the 5 µm fraction.

Cytb messenger RNA was short-lived, and eNA decay was biphasic

We detected dolphin-derived eDNA and 16S ribosomal eRNA across multiple timepoints, with signals persisting up to 48 hours after the start of the experiment. In contrast, Cytochrome b (Cytb) messenger eRNA was only detected in the first pre-transport sample (Figures 3, S4). This signal was lost during the ~3-hour transport period, and no Cytb emRNA was detected in subsequent laboratory samples, suggesting extremely rapid degradation.

Beyond this specific marker behavior, we observed that environmental nucleic acids (eNA) generally followed a biphasic decay pattern. This was especially clear for short eDNA fragments, which showed a steep decline within the first 48 hours, followed by a plateau phase in which low concentrations persisted through the end of the 7-day experiment. To formalize this observation, we compared six candidate decay models (Supplement), and the biphasic exponential model provided the best fit to the data based on leave-one-out cross-validation (Table S3).

Decay rate estimates varied by marker (Table 3). Although Cytb emRNA showed the fastest apparent initial decay (λ_1 = 1.525 hr^{-1}), this estimate is based on a single detection and subsequent non-detections, and should be interpreted with caution. Among consistently detected markers, 16S erRNA had the highest initial decay rate (λ_1 = 0.125 hr^{-1}; Figure 3B).

For eDNA, molecular length was a strong predictor of persistence (Figure 3A). Shorter targets, such as Cytb (λ_1 = 0.083 hr^{-1}), decayed more slowly, while longer targets like the Bridge fragment spanning 16S and D-loop (λ_1 = 0.121 hr^{-1}) decayed faster. Notably, the decay rates of the Bridge and 16S erRNA overlapped (Table 3), suggesting similar dynamics despite different molecular types.

The transition between the two decay phases consistently fell between 48 and 96 hours. However, because the biphasic model was fit jointly across all markers, it may have imposed a biphasic structure even on markers that lacked strong individual support for such a pattern—particularly 16S erRNA and Bridge eDNA. For these targets, the model estimated high second-phase decay rates likely reflect a lack of detections after the transition point, rather than true biphasic persistence. Verifying whether these rapidly degrading targets truly exhibit biphasic decay would require higher initial concentrations to enable detection beyond the early decay phase.

Table 3: Posterior decay rates estimated across markers. "λ_1" is the decay rate for the first phase of the exponential decay; "λ_1 2.5%" and "λ_1 97.5%" represent it's 95% confidence interval; "t_x" is the time break at which the decay rate was found to change from the first phase to the second; and "λ_2" is the decay rate for the second phase of the exponential decay. NA values indicate no detections were made at the relevant timepoint, making values unidentifiable.

Marker	λ_1	λ_1 2.5%	λ_1 97.5%	t_x	λ_2
Cytb eDNA	0.083 hr^{-1}	0.080 hr^{-1}	0.085 hr^{-1}	66 hrs	0.018 hr^{-1}
Cytb emRNA	1.525 hr^{-1}	0.903 hr^{-1}	2.320 hr^{-1}	NA	NA
16S eDNA	0.105 hr^{-1}	0.102 hr^{-1}	0.107 hr^{-1}	54 hrs	0.027 hr^{-1}
16S erRNA	0.125 hr^{-1}	0.111 hr^{-1}	0.141 hr^{-1}	50 hrs	0.394 hr^{-1}
Dloop eDNA	0.107 hr^{-1}	0.103 hr^{-1}	0.110 hr^{-1}	55 hrs	0.021 hr^{-1}
Bridge eDNA	0.121 hr^{-1}	0.112 hr^{-1}	0.130 hr^{-1}	48 hrs	0.293 hr^{-1}

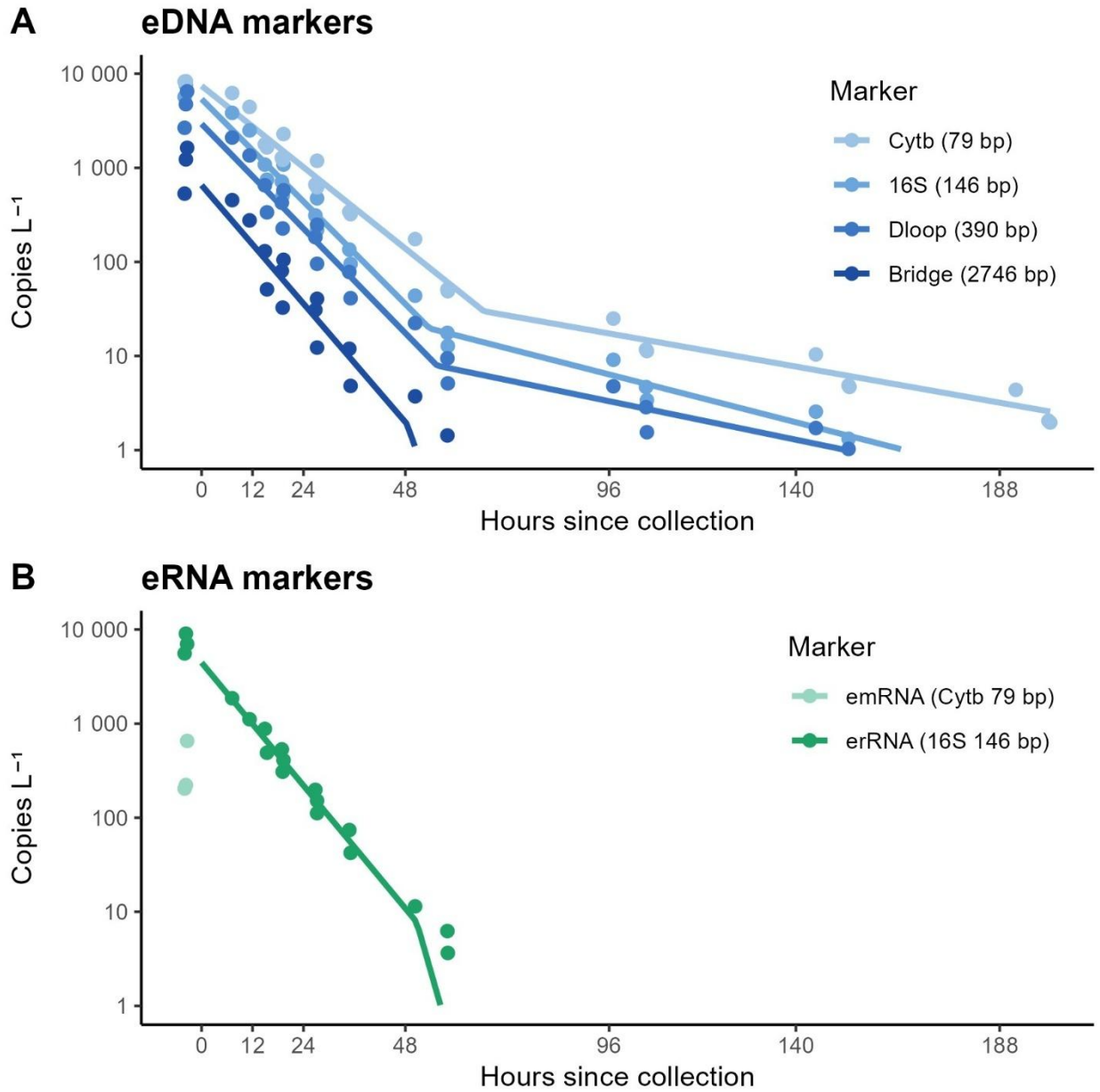

Figure 3: Biphasic-model decay of dolphin environmental nucleic acids (eNAs). (A) Mitochondrial DNA targets. (B) RNA targets. Solid lines are the posterior mean trajectories from the biphasic Bayesian ddPCR model; filled circles are the model-predicted concentrations at each sampling time for every biological replicate (three carboys). Colors distinguish markers and correspond to amplicon length: Cyt b 79 bp, 16 S 146 bp, DLL1 390 bp, and the 2 746 bp Bridge (DNA); Cyt b emRNA 79 bp and 16 S erRNA 146 bp (RNA). Axes are log-scaled; concentrations are expressed as copies L^{-1}.

402 **DISCUSSION**

403 This study provides the first empirical estimates of decay rates for multiple
404 environmental nucleic acid (eNA) components derived from a marine mammal. Using a
405 controlled experiment with seawater from a dolphin enclosure, we documented the
406 degradation of mitochondrial eDNA fragments of different lengths, ribosomal eRNA, and
407 messenger eRNA from *Tursiops truncatus* over seven days. We found that decay patterns
408 were highly dependent on molecule type and length, with messenger RNA degrading the
409 fastest, ribosomal RNA decaying slightly faster than its DNA counterpart, and longer DNA
410 fragments decaying more rapidly than shorter ones. Across most targets, decay followed a
411 biphasic trajectory, with a steep initial decline and a slower second phase. These results
412 confirm that eNA components differ markedly in environmental stability and underscore the
413 potential of combining multiple markers to improve the temporal resolution of eNA-based
414 detections.

415 **Rethinking molecular strategies for eDNA age estimation**

416 The ratio between eDNA and emRNA has been proposed as a molecular proxy for
417 time since eDNA shedding (Marshall et al., 2021), consistent with the spatiotemporally
418 variable eDNA composition hypothesis (Brandão-Dias et al., 2023). This approach assumes
419 that RNA decays more rapidly than DNA, such that high RNA:DNA ratios indicate recent
420 activity. However, our results suggest that messenger RNA (emRNA) is not well-suited for this
421 application in marine systems. Cytb emRNA was only detectable at the initial timepoint and
422 degraded beyond detection during transport—highlighting the molecule's extreme lability.
423 Similar challenges have been noted in other marine studies, where emRNA is often either
424 undetectable or not measurably different in decay from eDNA (Macher et al., 2024; Wood et
425 al., 2020). Beyond this, emRNA analysis requires transcript-specific assays, rapid
426 stabilization, and higher-cost laboratory workflows (Parsley & Goldberg, 2023; Yates et al.,
427 2021), which limit its practicality for most field applications.

428 Instead, our findings support the use of eDNA fragment length as a proxy for
429 degradation state. Longer mitochondrial markers decayed consistently faster than shorter
430 ones, as shown here and in prior work (Brandão-Dias et al., 2025; Hirohara et al., 2021),
431 making them well-suited for relative age estimation (T. Jo, Murakami, et al., 2020). This
432 method is logistically simple—relying on standard eDNA workflows and multiplexed
433 assays—and broadly applicable across taxa and systems. Importantly, quantitative
434 estimation of eDNA age requires both accurate decay rates and knowledge of the initial
435 proportion of each component, so that their relative abundance over time can be
436 meaningfully interpreted (Hallack et al., under review). When targeting mitochondrial loci,
437 the physical linkage of gene regions provides a useful simplification: short and long

438 fragments are expected to originate at roughly equal copy number, enabling decay-based
439 inferences without requiring independent normalization of starting ratios. On the other hand,
440 because mRNA expression levels change by context, the starting proportion between mRNA
441 and DNA in environmental samples will always vary, and initial proportions cannot be
442 accurately established.

443 Thus, pairing mitochondrial markers of different lengths offers a scalable, cost-
444 effective alternative to RNA-based strategies. Rather than relying on a single target, a duplex
445 assay can be designed to simultaneously amplify two mitochondrial regions with a
446 deliberate difference in length—maximizing the contrast in decay rates while maintaining
447 amplification efficiency. While this approach still requires well-characterized decay
448 dynamics and careful assay design, it circumvents the preservation challenges, higher
449 analysis costs, transcriptomic variability, and limited detectability that constrain the use of
450 emRNA. Thus, as eDNA-based surveys push toward finer spatiotemporal resolution,
451 fragment-length-based mitochondrial assays offer a practical framework for estimating the
452 age of detections in aquatic systems.

453 **Distinguishing Ribosomal and Messenger eRNA in Environmental Studies**

454 In our study, we found cytochrome b (Cytb) messenger eRNA (emRNA) at very low
455 concentrations, detectable only at the initial time point before water samples were
456 transferred to the environmental chamber. Low levels of Cytb emRNA in environmental
457 samples has been found in other studies (Jo et al., 2024), and these low concentrations are
458 the likely explained by low generation and expression of Cytb from eNA-generating tissue. In
459 contrast, ribosomal eRNA (erRNA) was present at much higher concentrations in our
460 samples, consistent with its constitutive expression, and decayed only slightly faster than
461 its equivalent DNA. This contrast in stability and concentrations of both forms of RNA aligns
462 with well-documented differences in RNA stability from forensic and molecular biology
463 research, where ribosomal RNA's secondary structure may protect it from degradation
464 (Houseley & Tollervey, 2009; Sidova et al., 2015). These findings highlight a fundamental
465 distinction between erRNA and emRNA: while erRNA in found in high concentrations and
466 can be reliably detected, emRNA is highly transient, making it a good candidate for detection
467 of more recent targets, but potentially unreliable in yielding consistent taxa detections given
468 its low starting concentrations.

469 The rapid degradation of mRNA is associated with its biological function. Within cells,
470 mRNA is a highly labile molecule that allows for rapid and dynamic gene expression
471 regulation (Sachs, 1993). To maintain precise control over protein synthesis, cells possess
472 multiple pathways for degrading mRNA efficiently, including exonuclease-mediated decay
473 and other complex biomolecular pathways (Belasco & Brawerman, 2012; Shyu et al., 2008).

Additionally, mRNA's single-stranded structure and chemical composition (i.e., an extra hydroxyl group) make it inherently less stable than DNA, leading to its rapid degradation both within cells and in the environment, particularly in high temperatures and alkaline conditions (T. Jo et al., 2023; Li & Breaker, 1999). In contrast, rRNA is constitutively (permanently) expressed in large quantities, representing over 80% of all RNA within cells in many estimates, and plays a structural role in ribosome assembly (Blanco & Blanco, 2017; Lewis & Tollervey, 2000; Warner, 1999). Its highly structured secondary and tertiary conformations enhance its resistance to enzymatic degradation (Sidova et al., 2015; Zhang et al., 2021), which likely extends to higher stability in the environment as well.

Despite these well-established molecular differences, the term "eRNA" is often used interchangeably in the eDNA literature to refer to both erRNA and emRNA, despite their fundamentally different properties. This conflation can lead to incorrect assumptions about eRNA persistence, decay rates, and ecological interpretability. Specifically, our results and previous literature indicate that emRNA degrades much faster than eDNA in environmental samples, and its initial concentration depends heavily on gene expression in the tissues shedding eDNA. Because gene expression varies across tissues, developmental stages, and environmental conditions, interpreting emRNA abundance requires transcriptomic knowledge of the target species—information that is often unavailable, but can be used to inform emRNA assay development (Parsley & Goldberg, 2023). Consequently, assays designed for both eDNA and emRNA detection (e.g., targeting Cytb, as tested here) may not be widely effective, as the emRNA marker will have to be customized for each application.

In contrast, erRNA is more abundant, making it a more stable biomarker but unsuitable for most other applications where emRNA would be advantageous over eDNA, such as metabolic inferences (Yates et al., 2021). Supporting this, previous metabarcoding studies using erRNA and eDNA to detect species with a 12S marker found minimal differences in detection rates, though erRNA showed faster species accumulation curves (Littlefair et al., 2022; Macher et al., 2024). Macher et al. (2024) also tested emRNA-based detection using cytochrome oxidase I (COI), and as expected, emRNA was less effective than eDNA in species detection due to its rapid degradation (see above). However, its faster decay resulted in stronger spatiotemporal patterns, reflecting its short-lived nature in the environment.

These findings reinforce the importance of distinguishing rRNA from mRNA in environmental studies. The ecological patterns observed for rRNA cannot be assumed to apply to mRNA, and vice versa. Given their fundamental biological and functional differences, treating both molecules collectively as "eRNA" is misleading and can obscure key differences in their degradation rates and interpretability in environmental monitoring.

510 Future research should clarify this distinction and ensure that eRNA studies account for the
511 vastly different behaviors of these two RNA types in environmental contexts.

512 **Dolphin eDNA Predominantly Retained in Large Particle Fractions**

513 Interestingly, we found that the vast majority of dolphin eDNA was captured on the
514 largest pore size filter (5 μm), with only residual amounts recovered in smaller size fractions
515 (Figure 2). This pattern contrasts with previous studies on the particle size distribution (PSD)
516 of eDNA from other marine taxa, such as teleost fish (Jo et al., 2019) and elasmobranchs
517 (Cooper et al., 2022), whose eDNA is more evenly distributed down to small filter pore sizes
518 (< 1 μm). While eDNA PSD is known to vary with environmental conditions and organism
519 (Barnes et al., 2021; Zhao et al., 2021), the pattern observed here closely resembles that
520 reported for freshwater fish in the presence of clay or titanium dioxide, which strongly adsorb
521 to eDNA (Brandão-Dias et al., 2023). However, such particles were not present in our
522 samples in substantial quantities. There are two possible alternative explanations for the
523 observed PSD. First, it is possible that filtration failure occurred at the smaller pore sizes,
524 preventing accurate capture of eDNA in those fractions. Nonetheless, we observed the same
525 pattern across three replicate carboys, which were filtered separately. Alternatively, if
526 experimental error can be excluded, the results may indicate that marine mammal eNA is
527 predominantly associated with larger particles—possibly due to tissue origin, mucus
528 binding, or aggregation. If this is the case, it has important implications for sampling design:
529 using larger pore size filters may enhance eDNA yield and improve detection probability for
530 marine mammals by allowing greater volumes to be processed.

531 **Carryover DNA and components of eDNA**

532 Commercially available extractions columns were originally designed to extract high
533 molecular yield DNA from tissue samples. However, they have been commonly used for
534 extracting eDNA from filters over the past two decades and have yielded sufficient DNA for
535 most applications (Takahashi et al., 2023). To our knowledge, no other studies have
536 captured and quantified eDNA that passes through the DNA extraction columns to quantify
537 this inefficiency. Here, we found a substantial amount of eDNA passed through the initial
538 column, largely comprising shorter DNA molecules as measured by a TapeStation
539 (Supplement Figure 2). This finding points to a potential blind spot in many eDNA workflows:
540 studies seeking rare targets or high detection sensitivity should be cautious about relying on
541 column-based extraction methods, despite their convenience and scalability.

542 In addition to quantifying the amount of carryover eDNA, we also quantified the decay
543 rate of carryover eDNA with one marker (Cytb) and found it to decay significantly slower than
544 the eDNA fraction captured on the first extraction column (Figure S3). This is likely due to a

cascading effect, where the decay of longer eDNA molecules creates shorter eDNA molecules, resulting is a slower apparent decay of the smaller fragment size (Brandão-Dias et al., 2023). Nonetheless, it is unclear if this method of splitting eNA components (i.e., eDNA vs. carryover eDNA) will be useful in the future because the fraction of eNA passing through the first column may not be stable, and may vary substantially under varying total quantities of DNA in the sample and other chemical characteristics of the sample. Thus, while splitting eNA by molecule length (in basepairs) may find its applications, separation of multiple eNA components may be more reliable with other methods such as sequential filtration (Brandão-Dias et al., 2025; Turner et al., 2014), evaluating multiple markers of varying lengths as here, or differential extraction methods (Kirtane et al., 2023).

Mechanisms and practical significance of Biphasic decay

Dolphin eDNA in our experiment followed a biphasic exponential decay: a steep first-phase loss lasting ~48 h, followed by a low-level "tail" that persisted for days. Similar two-phase kinetics have been reported from rivers, lakes, and coastal waters (e.g. Andruszkiewicz Allan et al., 2021; T. S. Jo, 2023; Shogren et al., 2018), but often go unrecognized when decay experiments end after only one or two days (e.g. Sassoubre et al., 2016; Snyder et al., 2023). We detected no compelling biphasic signal for either ribosomal or messenger eRNA, but it is possible RNA also follows the same pattern.

The processes that generate two-phase decay remain unresolved. Three non-exclusive explanations have been previously proposed: (i) physical shielding, in which DNA adsorbed to mineral or organic particles become inaccessible to nucleases (Barnes et al., 2021; Cai et al., 2006); (ii) encapsulation, whereby intact cells and mitochondria only release DNA after membrane rupture (Moushomi et al., 2019; Torti et al., 2015); and (iii) particle-size-dependent removal, where large aggregates settle or are grazed quickly while finer particles or dissolved DNA persist in suspension (Torti et al., 2015). Given these mechanisms are associated with different eDNA states, disentangling them will require experiments that characterize or separate DNA states.

Nonetheless, from a monitoring perspective, the slow second phase probably contributes little to routine eDNA surveys: most metabarcoding data will be dominated by the highly concentrated but rapidly decaying fraction, as the residual tail is easily swamped by fresh inputs. Nevertheless, understanding the process could improve source-age estimates, especially when low concentrations are observed.

ACKNOWLEDGEMENTS:

The authors thank the U.S. Naval Base Kitsap-Bangor for logistic support, Kate Bertko for administrative and field support, Krista Nichols, Amy Van Cise, Elizabeth Brasseale, and Olivia Scott for field sampling support, and Andrew Olaf Shelton for sampling support and assistance discussing the STAN decay model. This research was funded by the Office of Naval Research under Award Number (N00014-22-1-2719) and supported through collaborative research efforts with the U.S. Navy's Marine Mammals Program. Any use of trade, firm, or product names is for descriptive purposes only and does not imply endorsement by the U.S. Government.

REFERENCES

Allan, E. A., DiBenedetto, M. H., Lavery, A. C., Govindarajan, A. F., & Zhang, W. G. (2021). Modeling characterization of the vertical and temporal variability of environmental DNA in the mesopelagic ocean. *Scientific Reports*, *11*(1), 21273. https://doi.org/10.1038/s41598-021-00288-5

Andruszkiewicz Allan, E., Zhang, W. G., C. Lavery, A., & F. Govindarajan, A. (2021). Environmental DNA shedding and decay rates from diverse animal forms and thermal regimes. *Environmental DNA*, *3*(2), 492–514. https://doi.org/10.1002/edn3.141

Baker, C. S., Steel, D., Nieukirk, S., & Klinck, H. (2018). Environmental DNA (eDNA) From the Wake of the Whales: Droplet Digital PCR for Detection and Species Identification. *Frontiers in Marine Science*, *5*. https://doi.org/10.3389/fmars.2018.00133

Barnes, M. A., Chadderton, W. L., Jerde, C. L., Mahon, A. R., Turner, C. R., & Lodge, D. M. (2021). Environmental conditions influence eDNA particle size distribution in aquatic systems. *Environmental DNA*, *3*(3), 643–653. https://doi.org/10.1002/edn3.160

Barnes, M. A., & Turner, C. R. (2016). The ecology of environmental DNA and implications for conservation genetics. *Conservation Genetics*, *17*(1), 1–17. https://doi.org/10.1007/s10592-015-0775-4

Barnes, M. A., Turner, C. R., Jerde, C. L., Renshaw, M. A., Chadderton, W. L., & Lodge, D. M. (2014). Environmental Conditions Influence eDNA Persistence in Aquatic Systems. *Environmental Science & Technology*, *48*(3), 1819–1827. https://doi.org/10.1021/es404734p

Belasco, J. G., & Brawerman, G. (2012). *Control of Messenger RNA Stability*. Elsevier.

Blanco, A., & Blanco, G. (2017). Chapter 6—Nucleic Acids. In A. Blanco & G. Blanco (Eds.), *Medical Biochemistry* (pp. 121–140). Academic Press. https://doi.org/10.1016/B978-0-12-803550-4.00006-9

Bowers, H. A., Pochon, X., von Ammon, U., Gemmell, N., Stanton, J.-A. L., Jeunen, G.-J., Sherman, C. D. H., & Zaiko, A. (2021). Towards the Optimization of eDNA/eRNA Sampling Technologies for Marine Biosecurity Surveillance. *Water*, *13*(8), Article 8. https://doi.org/10.3390/w13081113

Brandão-Dias, P. F. . P., Tank, J. L., Snyder, E. D., Mahl, U. H., Peters, B., Bolster, D., Shogren, A. J., Lamberti, G. A., Bibby, K., & Egan, S. P. (2023). Suspended Materials Affect Particle Size Distribution and Removal of Environmental DNA in Flowing Waters. *Environmental Science & Technology*, *57*(35), 13161–13171. https://doi.org/10.1021/acs.est.3c02638

Brandão-Dias, P. F. P., Hallack, D. M. C., Snyder, E. D., Tank, J. L., Bolster, D., Volponi, S., Shogren, A. J., Lamberti, G. A., Bibby, K., & Egan, S. P. (2023). Particle size influences

decay rates of environmental DNA in aquatic systems. *Molecular Ecology Resources*, *23*(4), 756–770. https://doi.org/10.1111/1755-0998.13751

Brandão-Dias, P. F. P., Snyder, E., Tank, J. L., Mahl, U. H., Peters, B., Shogren, A. J., Bolster, D., Lamberti, G. A., Bibby, K., & Egan, S. P. (2025). Comparing the Fate of eDNA by Particle Sizes and Molecule Lengths in Recirculating Streams. *Environmental DNA*, *7*(2), e70066. https://doi.org/10.1002/edn3.70066

Bylemans, J., Furlan, E. M., Gleeson, D. M., Hardy, C. M., & Duncan, R. P. (2018). Does Size Matter? An Experimental Evaluation of the Relative Abundance and Decay Rates of Aquatic Environmental DNA. *Environmental Science & Technology*, *52*(11), 6408–6416. https://doi.org/10.1021/acs.est.8b01071

Cai, P., Huang, Q.-Y., & Zhang, X.-W. (2006). Interactions of DNA with Clay Minerals and Soil Colloidal Particles and Protection against Degradation by DNase. *Environmental Science & Technology*, *40*(9), 2971–2976. https://doi.org/10.1021/es0522985

Carpenter, B., Gelman, A., Hoffman, M. D., Lee, D., Goodrich, B., Betancourt, M., Brubaker, M., Guo, J., Li, P., & Riddell, A. (2017). Stan: A Probabilistic Programming Language. *Journal of Statistical Software*, *76*, 1–32. https://doi.org/10.18637/jss.v076.i01

Cooper, M. K., Villacorta-Rath, C., Burrows, D., Jerry, D. R., Carr, L., Barnett, A., Huveneers, C., & Simpfendorfer, C. A. (2022). Practical eDNA sampling methods inferred from particle size distribution and comparison of capture techniques for a Critically Endangered elasmobranch. *Environmental DNA*, *4*(5), 1011–1023. https://doi.org/10.1002/edn3.279

Guri, G., Ray, J. L., Shelton, A. O., Kelly, R. P., Præbel, K., Andruszkiewicz Allan, E., Yoccoz, N., Johansen, T., Wangensteen, O. S., Hanebrekke, T., & Westgaard, J.-I. (2024). Quantifying the Detection Sensitivity and Precision of qPCR and ddPCR Mechanisms for eDNA Samples. *Ecology and Evolution*, *14*(12), e70678. https://doi.org/10.1002/ece3.70678

Harrison, J. B., Sunday, J. M., & Rogers, S. M. (2019). Predicting the fate of eDNA in the environment and implications for studying biodiversity. *Proceedings of the Royal Society B: Biological Sciences*, *286*(1915), 20191409. https://doi.org/10.1098/rspb.2019.1409

Hindson, C. M., Chevillet, J. R., Briggs, H. A., Gallichotte, E. N., Ruf, I. K., Hindson, B. J., Vessella, R. L., & Tewari, M. (2013). Absolute quantification by droplet digital PCR versus analog real-time PCR. *Nature Methods*, *10*(10), 1003–1005. https://doi.org/10.1038/nmeth.2633

Hirohara, T., Tsuri, K., Miyagawa, K., Paine, R. T. R., & Yamanaka, H. (2021). The Application of PMA (Propidium Monoazide) to Different Target Sequence Lengths of Zebrafish eDNA: A New Approach Aimed Toward Improving Environmental DNA Ecology and Biological Surveillance. *Frontiers in Ecology and Evolution*, *9*. https://www.frontiersin.org/articles/10.3389/fevo.2021.632973

Houseley, J., & Tollervey, D. (2009). The Many Pathways of RNA Degradation. *Cell*, *136*(4), 763–776. https://doi.org/10.1016/j.cell.2009.01.019

Jerde, C. L., Mahon, A. R., Chadderton, W. L., & Lodge, D. M. (2011). “Sight-unseen” detection of rare aquatic species using environmental DNA: eDNA surveillance of

670 rare aquatic species. *Conservation Letters*, *4*(2), 150–157.
671 https://doi.org/10.1111/j.1755-263X.2010.00158.x
672 Jo, T., Arimoto, M., Murakami, H., Masuda, R., & Minamoto, T. (2019). Particle Size
673 Distribution of Environmental DNA from the Nuclei of Marine Fish. *Environmental*
674 *Science & Technology*, *53*(16), 9947–9956. https://doi.org/10.1021/acs.est.9b02833
675 Jo, T., Arimoto, M., Murakami, H., Masuda, R., & Minamoto, T. (2020). Estimating shedding
676 and decay rates of environmental nuclear DNA with relation to water temperature
677 and biomass. *Environmental DNA*, *2*(2), 140–151. https://doi.org/10.1002/edn3.51
678 Jo, T., Murakami, H., Masuda, R., & Minamoto, T. (2020). Selective collection of long
679 fragments of environmental DNA using larger pore size filter. *Science of The Total*
680 *Environment*, *735*, 139462. https://doi.org/10.1016/j.scitotenv.2020.139462
681 Jo, T., Murakami, H., Masuda, R., Sakata, M. K., Yamamoto, S., & Minamoto, T. (2017). Rapid
682 degradation of longer DNA fragments enables the improved estimation of
683 distribution and biomass using environmental DNA. *Molecular Ecology Resources*,
684 *17*(6). https://doi.org/10.1111/1755-0998.12685
685 Jo, T. S. (2023). Factors affecting biphasic degradation of eDNA released by Japanese jack
686 mackerel (*Trachurus japonicus*). *Journal of Experimental Marine Biology and*
687 *Ecology*, *568*, 151941. https://doi.org/10.1016/j.jembe.2023.151941
688 Jo, T. S., Ozaki, Y., Matsuda, N., & Yamanaka, H. (2024). Assessment of Allometry in
689 Environmental DNA and RNA Production From Ayu (Plecoglossus altivelis) in an
690 Experimental Condition Using Mitochondrial and Nuclear Gene Markers.
691 *Environmental DNA*, *6*(6), e70052. https://doi.org/10.1002/edn3.70052

Jo, T., Tsuri, K., Hirohara, T., & Yamanaka, H. (2023). Warm temperature and alkaline conditions accelerate environmental RNA degradation. *Environmental DNA*, *5*(5), 836–848. https://doi.org/10.1002/edn3.334

Joseph, C., Faiq, M. E., Li, Z., & Chen, G. (2022). Persistence and degradation dynamics of eDNA affected by environmental factors in aquatic ecosystems. *Hydrobiologia*, *849*(19), 4119–4133. https://doi.org/10.1007/s10750-022-04959-w

Kagzi, K., Hechler, R. M., Fussmann, G. F., & Cristescu, M. E. (2022). Environmental RNA degrades more rapidly than environmental DNA across a broad range of pH conditions. *Molecular Ecology Resources*, *22*(7), 2640–2650. https://doi.org/10.1111/1755-0998.13655

Kirtane, A., Kleyer, H., & Deiner, K. (2023). Sorting states of environmental DNA: Effects of isolation method and water matrix on the recovery of membrane-bound, dissolved, and adsorbed states of eDNA. *Environmental DNA*, *5*(3), 582–596. https://doi.org/10.1002/edn3.417

Lamb, P. D., Fonseca, V. G., Maxwell, D. L., & Nnanatu, C. C. (2022). Systematic review and meta-analysis: Water type and temperature affect environmental DNA decay. *Molecular Ecology Resources*, *22*(7), 2494–2505. https://doi.org/10.1111/1755-0998.13627

Lewis, J. D., & Tollervey, D. (2000). Like Attracts Like: Getting RNA Processing Together in the Nucleus. *Science*, *288*(5470), 1385–1389. https://doi.org/10.1126/science.288.5470.1385

Li, Y., & Breaker, R. R. (1999). Kinetics of RNA Degradation by Specific Base Catalysis of Transesterification Involving the 2‘-Hydroxyl Group. *Journal of the American Chemical Society*, *121*(23), 5364–5372. https://doi.org/10.1021/ja990592p

Louis, M., Korlević, P., Nykänen, M., Archer, F., Berrow, S., Brownlow, A., Lorenzen, E. D., O’Brien, J., Post, K., Racimo, F., Rogan, E., Rosel, P. E., Sinding, M.-H. S., van der Es, H., Wales, N., Fontaine, M. C., Gaggiotti, O. E., & Foote, A. D. (2023). Ancient dolphin genomes reveal rapid repeated adaptation to coastal waters. *Nature Communications*, *14*(1), 4020. https://doi.org/10.1038/s41467-023-39532-z

Macher, T.-H., Arle, J., Beermann, A. J., Frank, L., Hupało, K., Koschorreck, J., Schütz, R., & Leese, F. (2024). Is it worth the extra mile? Comparing environmental DNA and RNA metabarcoding for vertebrate and invertebrate biodiversity surveys in a lowland stream. *PeerJ*, *12*, e18016. https://doi.org/10.7717/peerj.18016

Marshall, N. T., Vanderploeg, H. A., & Chaganti, S. R. (2021). Environmental (e)RNA advances the reliability of eDNA by predicting its age. *Scientific Reports*, *11*(1), 2769. https://doi.org/10.1038/s41598-021-82205-4

Mauvisseau, Q., Harper, L., Sander, M., Hanner, R. H., Kleyer, H., & Deiner, K. (2021). *The multiple states of environmental DNA and what is known about their persistence in aquatic environments* [Preprint]. Preprints. https://doi.org/10.22541/au.163638394.41572509/v1

Miyata, K., Inoue, Y., Amano, Y., Nishioka, T., Yamane, M., Kawaguchi, T., Morita, O., & Honda, H. (2021). Fish environmental RNA enables precise ecological surveys with

high positive predictivity. *Ecological Indicators*, *128*, 107796. https://doi.org/10.1016/j.ecolind.2021.107796

Moushomi, R., Wilgar, G., Carvalho, G., Creer, S., & Seymour, M. (2019). Environmental DNA size sorting and degradation experiment indicates the state of Daphnia magna mitochondrial and nuclear eDNA is subcellular. *Scientific Reports*, *9*(1), 12500. https://doi.org/10.1038/s41598-019-48984-7

Nagler, M., Podmirseg, S. M., Ascher-Jenull, J., Sint, D., & Traugott, M. (2022). Why eDNA fractions need consideration in biomonitoring. *Molecular Ecology Resources*, *22*(7), 2458–2470. https://doi.org/10.1111/1755-0998.13658

Parsley, M. B., & Goldberg, C. S. (2023). Environmental RNA can distinguish life stages in amphibian populations. *Molecular Ecology Resources*. https://onlinelibrary.wiley.com/doi/abs/10.1111/1755-0998.13857

Power, H., Takahashi, M., Jarman, S., & Berry, O. (2023). What is environmental DNA? *Environmental DNA*, *5*(6), 1743–1758. https://doi.org/10.1002/edn3.497

Qian, T., Shan, X., Wang, W., & Jin, X. (2022). Effects of Temperature on the Timeliness of eDNA/eRNA: A Case Study of Fenneropenaeus chinensis. *Water*, *14*(7), Article 7. https://doi.org/10.3390/w14071155

Sachs, A. B. (1993). Messenger RNA degradation in eukaryotes. *Cell*, *74*(3), 413–421. https://doi.org/10.1016/0092-8674(93)80043-E

Sampaio-Silva, F., Magalhães, T., Carvalho, F., Dinis-Oliveira, R. J., & Silvestre, R. (2013). Profiling of RNA Degradation for Estimation of Post Morterm Interval. *PLOS ONE*, *8*(2), e56507. https://doi.org/10.1371/journal.pone.0056507

Sassoubre, L. M., Yamahara, K. M., Gardner, L. D., Block, B. A., & Boehm, A. B. (2016). Quantification of Environmental DNA (eDNA) Shedding and Decay Rates for Three Marine Fish. *Environmental Science & Technology*, *50*(19), 10456–10464. https://doi.org/10.1021/acs.est.6b03114

Scriver, M., von Ammon, U., Pochon, X., Arranz, V., Stanton, J.-A. L., Gemmell, N. J., & Zaiko, A. (2024). Environmental DNA–RNA dynamics provide insights for effective monitoring of marine invasive species. *Environmental DNA*, *6*(2), e531. https://doi.org/10.1002/edn3.531

Scriver, M., Zaiko, A., Pochon, X., & von Ammon, U. (2023). Harnessing decay rates for coastal marine biosecurity applications: A review of environmental DNA and RNA fate. *Environmental DNA*, *5*(5), 960–972. https://doi.org/10.1002/edn3.405

Shogren, A. J., Tank, J. L., Egan, S. P., August, O., Rosi, E. J., Hanrahan, B. R., Renshaw, M. A., Gantz, C. A., & Bolster, D. (2018). Water Flow and Biofilm Cover Influence Environmental DNA Detection in Recirculating Streams. *Environmental Science & Technology*, *52*(15), 8530–8537. https://doi.org/10.1021/acs.est.8b01822

Shyu, A., Wilkinson, M. F., & van Hoof, A. (2008). Messenger RNA regulation: To translate or to degrade. *The EMBO Journal*, *27*(3), 471–481. https://doi.org/10.1038/sj.emboj.7601977

Sidova, M., Tomankova, S., Abaffy, P., Kubista, M., & Sindelka, R. (2015). Effects of *post-mortem* and physical degradation on RNA integrity and quality. *Biomolecular Detection and Quantification*, *5*, 3–9. https://doi.org/10.1016/j.bdq.2015.08.002

Snyder, E. D., Tank, J. L., Brandão-Dias, P. F. P., Bibby, K., Shogren, A. J., Bivins, A. W., Peters, B., Curtis, E. M., Bolster, D., Egan, S. P., & Lamberti, G. A. (2023). Environmental DNA (eDNA) removal rates in streams differ by particle size under varying substrate and light conditions. *Science of The Total Environment*, *903*, 166469. https://doi.org/10.1016/j.scitotenv.2023.166469

Suarez-Bregua, P., Álvarez-González, M., Parsons, K. M., Rotllant, J., Pierce, G. J., & Saavedra, C. (2022). Environmental DNA (eDNA) for monitoring marine mammals: Challenges and opportunities. *Frontiers in Marine Science*, *9*. https://doi.org/10.3389/fmars.2022.987774

Takahashi, M., Saccò, M., Kestel, J. H., Nester, G., Campbell, M. A., Van Der Heyde, M., Heydenrych, M. J., Juszkiewicz, D. J., Nevill, P., Dawkins, K. L., Bessey, C., Fernandes, K., Miller, H., Power, M., Mousavi-Derazmahalleh, M., Newton, J. P., White, N. E., Richards, Z. T., & Allentoft, M. E. (2023). Aquatic environmental DNA: A review of the macro-organismal biomonitoring revolution. *Science of The Total Environment*, *873*, 162322. https://doi.org/10.1016/j.scitotenv.2023.162322

Torti, A., Lever, M. A., & Jørgensen, B. B. (2015). Origin, dynamics, and implications of extracellular DNA pools in marine sediments. *Marine Genomics*, *24*, 185–196. https://doi.org/10.1016/j.margen.2015.08.007

Turner, C. R., Barnes, M. A., Xu, C. C. Y., Jones, S. E., Jerde, C. L., & Lodge, D. M. (2014). Particle size distribution and optimal capture of aqueous macrobial eDNA. *Methods in Ecology and Evolution*, *5*(7), 676–684. https://doi.org/10.1111/2041-210X.12206

Warner, J. R. (1999). The economics of ribosome biosynthesis in yeast. *Trends in Biochemical Sciences*, *24*(11), 437–440. https://doi.org/10.1016/S0968-0004(99)01460-7

Wood, S. A., Biessy, L., Latchford, J. L., Zaiko, A., von Ammon, U., Audrezet, F., Cristescu, M. E., & Pochon, X. (2020). Release and degradation of environmental DNA and RNA in a marine system. *Science of The Total Environment*, *704*, 135314. https://doi.org/10.1016/j.scitotenv.2019.135314

Xia, Z., Zhan, A., Gao, Y., Zhang, L., Haffner, G. D., & MacIsaac, H. J. (2018). Early detection of a highly invasive bivalve based on environmental DNA (eDNA). *Biological Invasions*, *20*(2), 437–447. https://doi.org/10.1007/s10530-017-1545-7

Xiong, J., MacCready, P., Brasseale, E., Andruszkiewicz Allan, E., Ramón-Laca, A., Parsons, K. M., Shaffer, M., & Kelly, R. P. (2025). Advective Transport Drives Environmental DNA Dispersal in an Estuary. *Environmental Science & Technology*, *59*(15), 7506–7516. https://doi.org/10.1021/acs.est.5c01286

Xiong, Y., Brandley, M. C., Xu, S., Zhou, K., & Yang, G. (2009). Seven new dolphin mitochondrial genomes and a time-calibrated phylogeny of whales. *BMC Evolutionary Biology*, *9*(1), 20. https://doi.org/10.1186/1471-2148-9-20

Yates, M. C., Derry, A. M., & Cristescu, M. E. (2021). Environmental RNA: A Revolution in Ecological Resolution? *Trends in Ecology & Evolution*, *36*(7), 601–609. https://doi.org/10.1016/j.tree.2021.03.001

Zhang, K., Hodge, J., Chatterjee, A., Moon, T. S., & Parker, K. M. (2021). Duplex Structure of Double-Stranded RNA Provides Stability against Hydrolysis Relative to Single-

Stranded RNA. *Environmental Science & Technology*, *55*(12), 8045–8053. https://doi.org/10.1021/acs.est.1c01255

Zhao, B., Van Bodegom, P. M., & Trimbos, K. (2021). The particle size distribution of environmental DNA varies with species and degradation. *Science of The Total Environment*, *797*, 149175. https://doi.org/10.1016/j.scitotenv.2021.149175